# Indirect Search Results for Signatures of Particle Dark Matter

*W. B. Atwood*

Santa Cruz Institute for Particle Physics Department of Physics
University of California
1156 High Street
Santa Cruz, 95064, USA

Recent astro-particle experiments have reported results of searches for signatures of particle dark matter (DM) other than the ubiquitious gravitational effects. Tantalizing hints of unexpected behavior in the cosmic-ray electron and positron spectra have been found by PAMELA, ATIC, and the *Fermi* LAT. However, these signatures, sometimes interpreted as coming from DM annihilation and/or decays, can have alternative – "standard" – astrophysical interpretations as well, and hence can be used to further constrain the mass, cross section, and distribution of DM. The forerunner experiment to the *Fermi* LAT, EGRET, detected excess diffuse $\gamma$-ray emission above 1 GeV, compared to standard astrophysical models for the diffuse Galactic $\gamma$-ray emission. However, this has not been confirmed by the *Fermi* LAT. Searches by the *Fermi* LAT for $\gamma$-rays from DM lines, clumps, and signals from nearby dwarf galaxies have also been performed. I will review the various experiments and discuss the new limits provided on the properties of particle DM.

## 1 Introduction

The existence of dark matter (DM) was first postulated by Zwicky and confirmed by astronomical rotation curves for stars within distant galaxies [1]. Stars at the periphery of galaxies have tangential velocities far in excess of that expected by estimating the gravitating mass of the galaxy within their orbits. And, this observation is repeated in essentially all galaxies for which this behavior has been looked for. More recently, in the collision of two galaxies known as the Bullet Cluster, the center of the luminous mass and the gravitational center are not co-located [2].

The existence of DM is not at issue, but rather its nature. The only observable trait found to date is the gravitational interaction. Many believe that this as-yet unobserved matter is particle in origin. Extensions to the Standard Model of particle physics often have enticing slots into which DM could fall, the idea being that it is a cosmological relic left over from the Big Bang. If indeed DM is particle in nature, then its interactions with ordinary matter as detailed by the Standard Model can be calculated. Signs of its presence could arise from either co-annihilation of two DM particles resulting in standard model particles, or these dark matter particles could simply decay into ordinary matter, albeit with a very long lifetime. A common expression for the resulting flux of $\gamma$-rays from DM particle co-annihilations is given by

$$F_\gamma(E,\psi) = \frac{<\sigma v>}{4\pi} \left[ \sum_f \frac{dN_f}{dE} B_f \right] \int_{l.o.s} \frac{1}{2} \left( \frac{\rho(l)}{M_\chi} \right)^2 dl \qquad (1)$$

where $F_\gamma$ is the flux of $\gamma$-rays, $<\sigma v>$ is the annihilation cross-section velocity average, the term in square brackets is the sum over possible final states where $B_f$ is the branching fraction and $dN_f/dE$ is the energy spectrum, and the integral in last term is along the line-of-sight for the observation with $\rho$ the DM energy density and $M_\chi$ the DM candidate mass. The ratio of the energy density to mass is the number density and the co-annihilation means this appears as a squared term in the expression. The uncertainties for the contributing terms in equation 1 are large, particularly the number density. State-of-the-art $N$-body simulations predict DM clumps over all length scales. Since the annihilation rate depends quadratically on the number density, clumping essentially boosts the potential signal. However, current simulations are numerically limited in resolution of the clumping below a lower length scale. Below this, the assumptions of the scaling behaviour of the clumping introduce a significant uncertainty in the annihilation rate that can be several orders of magnitude. For the case of decaying DM particles, the quadratic dependence on density becomes linear and in place of $\langle\sigma v\rangle$ is the DM particle decay rate.

The same expression can be written for final state particles other than $\gamma$-rays. Recent measurements of cosmic-ray (CR) fluxes of antiprotons, positrons, and electrons have provoked a great deal of speculation as to whether or not we are finally seeing evidence for the particle origins of the DM. I will first review the status of these CR searches and follow with $\gamma$-ray searches.

## 2 Cosmic-Ray Flux Measurements

The first experimental result to be discussed is the ATIC (Advanced Thin Ionization Calorimeter) collaboration's measurement of the total CR electron + positron flux [3]. This balloon-borne experiment has had four flights from the NSF Antarctic balloon facility. The original motivation for these measurements was to obtain the spectrum of entering CRs not only for electrons, but for protons and heavier nuclei as well. The detector was not tuned to provide a high discrimination power between electrons and hadrons. In particular, in order to insure that a large fraction of incoming nuclei energy would be deposited in the calorimeter section, about 1.5 radiation lengths of carbon served as a converter target in front of the calorimeter. This is contrary to the usual practice in a dedicated electron detector that tries to accentuate the separation between the first interaction locations of electrons and hadrons. A diagram of the ATIC detector is shown in Fig. 1.

The ATIC collaboration has logged four balloon flights to date, the third of these however ended prematurely and resulted in no useful data. Over the course of these flights the apparatus was upgraded, particularly the depth of the calorimeter which was increased from 18 to 22 radiation lengths for the fourth and last flight. In order to measure the electron spectrum, an offline analysis capable of discriminating between electrons and hadrons at greater then 1000:1 had to be achieved. Initially, the ATIC collaboration published the results for the first two balloon flights and more recently added the data from the last flight. The spectra, multiplied by $E^3$ to compress the dynamic range, is shown in Fig. 2.

The prominent enhancement in the spectrum around 600 GeV caused a great deal of excitement in 2008 and was interpreted in more than a few papers as a signature of particle

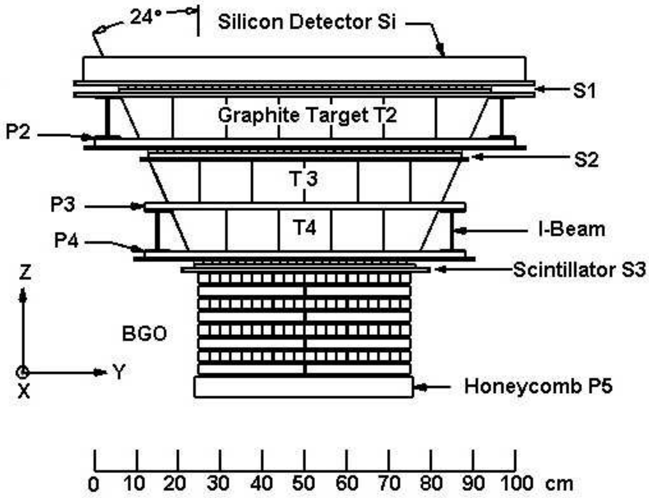


Figure 1: The ATIC detector. The top layer of silicon detectors is used to the determine the magnitude of the incoming charge. Three layers of graphite, interspersed with scintillation hodoscopes for tracking, enhance the early interaction of incoming hadronic CRs. A Bismuth-Germanium-Oxide calorimeter with 18–22 radiation lengths depth is located at the bottom of the instrument.

DM. However, it was also realized that the DM source for high-energy electrons would have to be quite close to the solar system, otherwise their energy would be significantly degraded via inverse Compton scattering of the interstellar radiation field and synchrotron cooling on the Galactic magnetic field.

During the same time period as the latter of the ATIC flights, a satellite-borne instrument has also been in operation: PAMELA, the Payload for Antimatter Matter Exploration and Light-nuclei Astrophysics[4]. The PAMELA apparatus distinguishes itself from other payloads by having a magnetic spectrometer that can determine the sign and magnitude of the charge of the incoming CRs. The primary motivation for PAMELA was to measure with high statistics the antimatter component in CRs. The relevance of PAMELA to DM searches is that annihilations (or decays) of DM particles will create equal amounts of matter and antimatter in the final state. A diagram of the PAMELA apparatus is shown in Fig. 3.

PAMELA was launched in June 2007 onboard a Russian satellite and has taken data continually since launch. The two results published in 2008 of interest for DM searches are shown in Fig. 4: the CR antiproton and positron fractions, respectively. The high statistics and energy coverage have resulted in a significant improvement for the measurements of these CR species.

The PAMELA measurement of the antiproton fraction is consistent with that expected from standard secondary production by CR nuclei interacting with the interstellar gas. The surprise was the dramatic rise in the positron fraction with increasing energy. This together with the ATIC results was the source of many papers in 2008. We currently await the publication of PAMELA results for the separate CR electron and positron spectra, which will provide deeper information than the positron fraction.

The newest experiment to provided data on the CR electron flux (hereafter I use the term

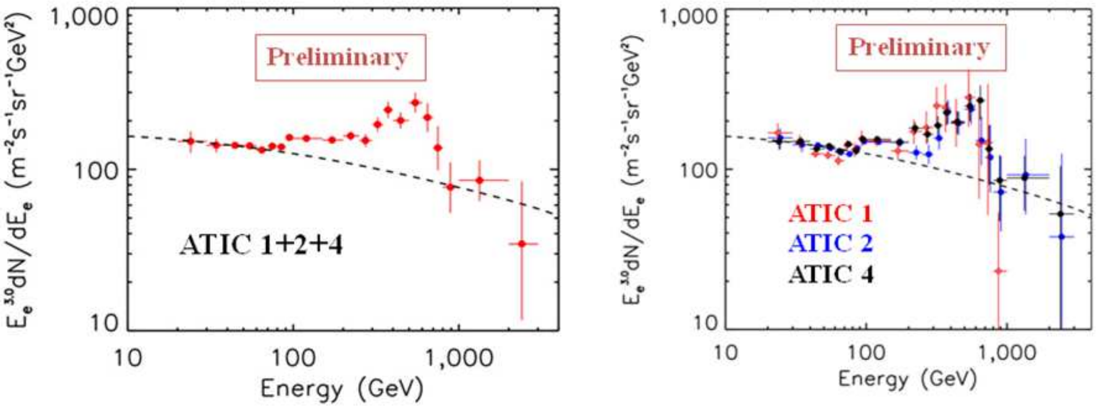


Figure 2: The total $e^+ + e^-$ spectrum measured by ATIC. The first and second flight (ATIC 1 & 2) showed an enhancement of $3.8\sigma$ centerd around 600 GeV. The fourth flight (ATIC 4) showed the same feature with increased statistics resulting in an overall significance of $5.1\sigma$.

"electron" to mean electrons and positrons combined) is the Large Area Telescope (LAT) on the *Fermi Gamma-ray Space Telescope*. This instrument was originally conceived in 1992 as the next generation high-energy $\gamma$-ray satellite as a follow on to the Energetic Gamma-Ray Experiment Telescope (EGRET) on the *Compton Gamma-Ray Observatory*. It was realized early in the evolution of the then named GLAST (Gamma-ray Large Area Telescope) project, that an excellent $\gamma$-ray instrument would also measure the CR electron component. After the *Fermi* launch in June, 2008, a dedicated effort was mounted to develop the electron measuring potential of this instrument. The LAT instrument along with the satellite and the companion Gamma ray Burst Monitor (GBM) is shown in Fig. 5. Details of the LAT can be found in reference[5].

The LAT is a pair-conversion telescope comprised of a $4 \times 4$ modular array with each module comprising a precision converter-tracker section followed by a calorimeter (see Fig. 5). The active elements of the tracker are silicon-strip detectors. The calorimeter is a hodoscopic configuration of 8.6 radiation lengths of CsI crystals that allows imaging of the shower development in the calorimeter. This imaging capability enables making corrections to the energy estimate for the shower leakage fluctuations event by event. The total thickness of the tracker and calorimeter is 10.1 radiation lengths at normal incidence. A segmented, anticoincidence detector (ACD) covers the tracker array, and a programmable trigger and data acquisition system uses prompt signals available from the tracker, calorimeter, and ACD to form a trigger that initiates readout of these three subsystems. The onboard trigger is optimized for rejecting events triggered by CR background particles while maximizing the number of events triggered by $\gamma$-rays, that are transmitted to the ground for further processing.

To take full advantage of the LATs large field-of-view (FoV), the primary observing mode of Fermi is the so-called "scanning mode". In this mode the instrument axis is pointed to $+35°$ from the zenith and towards one pole of the orbit on alternate orbits and to $-35°$ from the zenith for the other orbits. Thus, after two orbits (or about 3 hours for the nominal orbit at 565 km and 25.5° inclination) the sky exposure is almost uniform. For autonomous re-points or for other targets of opportunity, the observatory can be inertially pointed as well. Building on

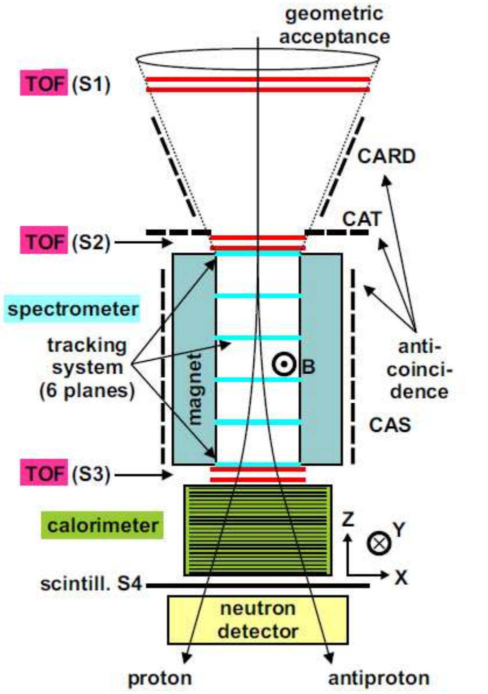


Figure 3: The PAMELA experiment. The magnetic spectrometer of this instrument is capable of of determining the sign of the charge of detected particles to energies $> 200$ GeV. PAMELA was launched in June 2007 onboard a Russian satellite and has taken data continually since launch.

the $\gamma$-ray analysis, the LAT Collaboration has developed an efficient electron detection strategy that provides sufficient background rejection for the measurement of the steeply falling electron spectrum up to 1 TeV[6]. Similar to ATIC, the LAT cannot directly distinguish electrons and positrons. Since the initial results above 20 GeV, the LAT results have been extended to below 10 GeV using an independent hardware trigger and analysis. Where the results overlap, the agreement is excellent. These results are shown in Fig. 6. Fits to this spectrum with a power law shows it falls with energy as $E^{-3.04}$ and does not exhibit prominent spectral features such as seen in the ATIC results. The energy resolution of the LAT calorimetry, verified by beam test and Monte Carlo, is sufficient that any prominent peak, such as seen by ATIC, would have been significantly detected by the analysis.

A standard diffusion-reacceleration CR propagation model [7, 8] based on the assumption that the CR electrons originate from a continuous distribution of sources, mainly associated with supernova remnants and pulsars, fits the LAT spectrum moderately well. This kind of model predicts a featureless spectrum from 10 GeV up to few hundreds of GeV. Above a few hundreds of GeV the assumptions for the sources in such a model break down. Due to the actual stochastic nature of CR electron sources in space and time, and to the strong synchrotron and inverse Compton energy losses, the spectrum should fall faster. Deviations from a featureless power law are likely to be caused by nearby sources [9, 11, 12, 13, 10]. The PAMELA results,

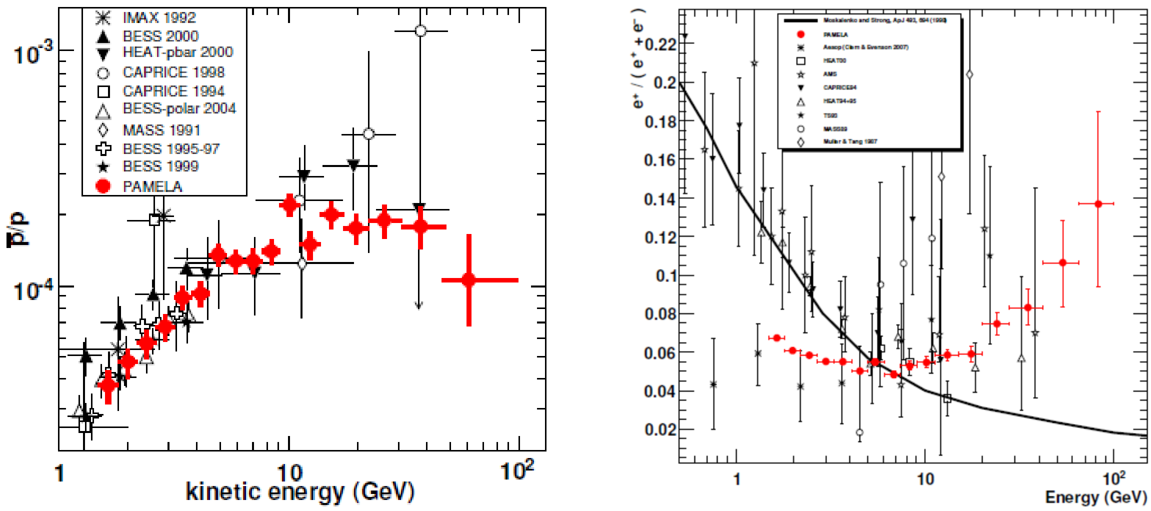


Figure 4: PAMELA results for the CR $\overline{p}/p$ ratio (left) and $e^+/(e^+ + e^-)$ ratio (right). Previous measurements are shown in black while the PAMELA data are shown in red. The dramatic improvement over earlier measurements is clear.

along with the Fermi and H.E.S.S. results [14, 15], may indicate the presence of a nearby primary source(s) of CR electrons and positrons, two classes of which stand out: nearby pulsar(s) [16, 11] and DM, either by annihilation [8] or decay, for example through grand unified interactions with a lifetime $\sim 10^{26}$ s [18].

## 3 Fermi-LAT Gamma-Ray Searches for Dark Matter

Gamma-ray signals from DM have been looked for using many different approaches with the first year of LAT data. These include searches for line signatures, excess emission from the Galactic Center, halo objects and galaxy clusters, together with studies of the diffuse Galactic and extragalactic $\gamma$-ray emission.

*Galactic Diffuse Emission:* The $\gamma$-ray sky is dominated by diffuse emission from the Milky Way. The diffuse Galactic emission (DGE) is generated by energetic CRs that interact with interstellar gas ($\pi^0$-decay and bremsstrahlung) and radiation fields (via inverse Compton scattering). An apparent excess in DGE spectrum was observed by EGRET $> 1$ GeV relative to conventional DGE models based on locally measured CR spectra [19]. The so-called EGRET "GeV excess" was proposed to be due to $\gamma$-rays from annihilating DM [20]. However, alternative explanations included variations in the CR spectra [12, 21] and instrumental effects [22, 23].

Based on analysis of data from the first year of observations, the *Fermi* LAT collaboration reported on measurements of the diffuse $\gamma$-ray emission from 100 MeV to 10 GeV for Galactic latitudes $10° \leq |b| \leq 20°$ [7]. The diffuse emission spectrum, shown in Fig. 7, is consistent with a DGE model that reproduces the local CR spectrum and does not require an additional component.

*Extra-Galactic Diffuse Emission:* The DGE presents a large forground signal to the much fainter

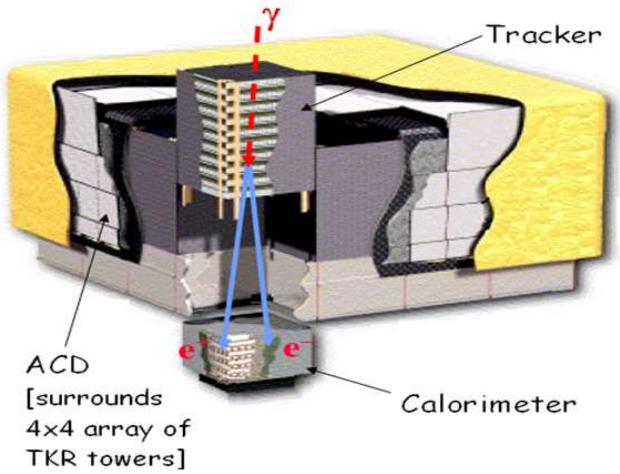


Figure 5: A cut-away diagram of the primary instrument on the *Fermi Gamma-ray Space Telescope*: the LAT. The LAT images the $\gamma$-ray sky in the energy band from $\sim$ 20 MeV to more than 300 GeV. The LAT is comprised of 16 indentical tracker/calorimeter modules arranged in a $4 \times 4$ array. The tracker portion of the instrument is covered by the anti-coincidence detector (ACD) comprised of 89 scintillation veto tiles. The ACD helps discriminate incoming charged particles from neutrals, such as $\gamma$-rays.

diffuse Extra-Galactic Gamma-ray Background (EGB). The EGB is the sum of contributions from unresolved sources and truly diffuse emssion processes, e.g., from ultra-high energy CRs interacting with background light, large-scale structure formation, etc., as well as possibly from cosmological DM through annihilation or decay. The LAT Collaboration has reported a measurement of the spectrum of the isotropic diffuse $\gamma$-ray radiation from 200 MeV to 100 GeV [25]. The biggest challenge in the determination of the EGB is the subtraction of the various foregrounds and this is the source of the largest systematic uncertainty. Most important are the contributions from the DGE, the instrumental background from misclassified CRs, and from the resolved sources. The mis-identified CRs are suppressed by applying very stringent event selection criteria albeit at the expense of efficiency. The DGE and the contribution from point sources is obtained from a fit to the *Fermi* LAT dataset. The derived spectrum is shown in Fig. 8. It is a featureless power law, significantly softer than the one obtained from EGRET observations [26]. Also, the spectrum does not show the feaure $\gtrsim 2$ GeV found in a reanalysis of the EGRET data with an updated diffuse model [27], that had been suggested as a DM signal [28].

*Dark Matter Line Searches:* Perhaps the cleanest and most convincing DM signal the LAT might measure would be a monochromatic $\gamma$-ray line-like feature sitting on top of some continuum spectrum. Such a feature would arise from two-body final states from DM particle annihilations into either a pair of $\gamma$-rays or a $\gamma$-ray and $Z^0$ boson. However, most estimates for the branching fraction into such states are very small ($< .001$) and place them well below the flux sensitivity of the LAT. A search for $\gamma$-ray lines has been done using the first year of data. Data from two regions of the sky have been used: Region A excludes the Galactic Plane ($|b| > 10°$) and Region B includes the inner Galaxy ($|l| < 30°$) along with Region A. The

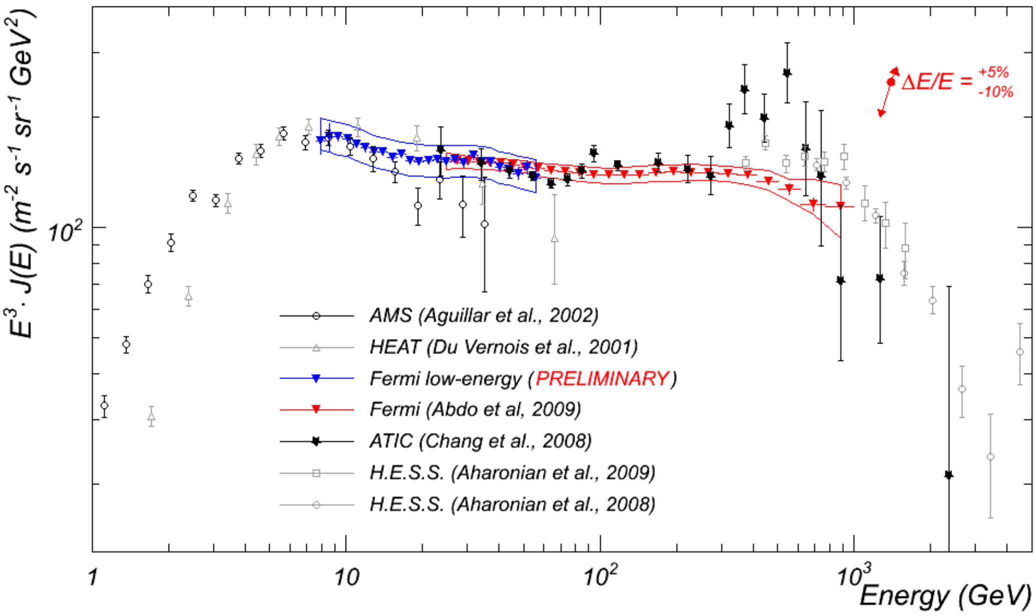


Figure 6: The Fermi-LAT measured total CR electron + positron spectrum (red and blue points). The two-headed arrow in the top-right corner of the figure gives the size and direction of the shift of the spectrum implied by a $+10\%/-5\%$ shift of the absolute energy scale of the LAT. This shift corresponds to the current estimate of the systematic uncertainty for the LAT energy scale.

motivation for Region B is this is where the largest concentration of DM is thought to be. After removing $\gamma$-rays from known sources by cutting out circular portions of the sky (ie., within $0.2°$ of the source position) the data was binned into energy intervals with relative widths of 20%. A line shape along with a polynomial background determined from the side bins is then fitted for each bin. No line signals have been found. Due to the large uncertainty in the branching fraction, this does not provide a significant result constraining the parameter space for DM models.

*The Galactic Center:* For the case of annihilating DM, the Galactic Center (GC) is a natural place to expect a large enhancement. Since the annihilation rate is proportional to the number density of the DM particles squared, and most particle DM models have the density increasing (sometime dramatically) in the vicinity of the GC, the potential signal would be strongest in this region. However the GC is a complex region with many nearby sources and a large DGE flux.

The LAT analysis uses data within $1°$ of the GC and is attempting to detect a spectral component the might be ascribed to DM annihilations. No attempt is made to subtract either the multitude of sources or the large DGE component. Fits are made to the spectra from this region using simple power laws, or broken power laws, as is common for standard astrophysical sources. These fits are compared to the same with an added DM spectral component determined from specific particle physics models (e.g., 50 GeV DM particles annihilating through the $b\bar{b}$–

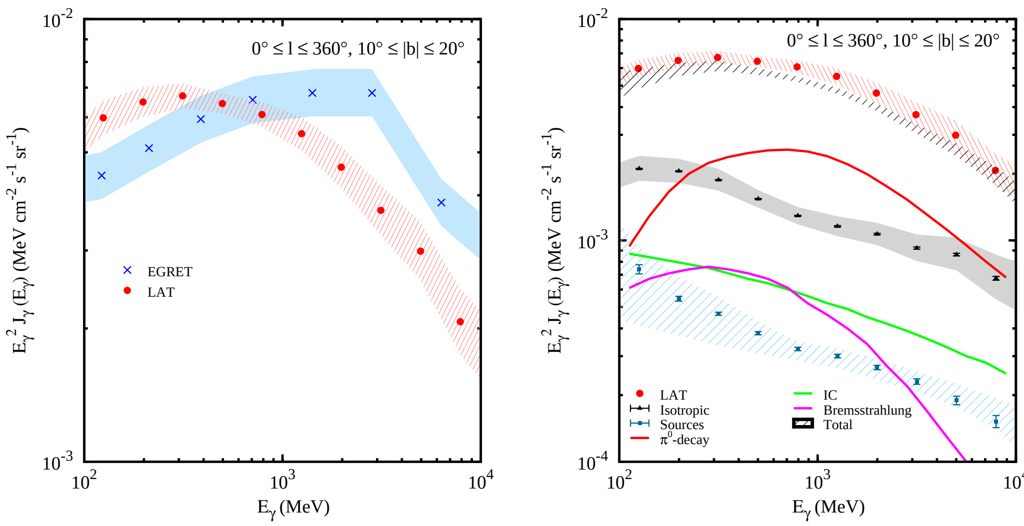


Figure 7: Diffuse emission intensity averaged over all Galactic longitudes for latitude range $10° \leq |b| \leq 20°$. Left panel: LAT (red dots) and EGRET (blue crosses) data. Systematic uncertainties: LAT, red; EGRET, blue. Right panel: LAT data with model, source, and unidentified background (UIB) components. Model (lines): $\pi^0$-decay, red; bremsstrahlung, magenta; IC, green. Shaded/hatched regions: UIB, grey/solid; source, blue/hatched; total (model + UIB + source), black/hatched. The UIB component was determined by fitting the data and sources with the model held constant using the latitude range $|b| \geq 30°$. For full details see [7].

quark channel). Typical broken power-law fits are adequate for this region to describe the combination of astrophysical sources and DGE, hence no spectral signature for DM annihilations (modulo the given assumptions) is claimed.

*Halo Objects:* There are two types of DM concentrations which have been searched for. The first are the dwarf spheroidal galaxies (dSphs) that circulate about the Milky Way and the second are DM clumps as predicted by various $N$-body simulations. The DM clumps are more speculative than the dSphs, since none have actually been observed in other wavebands, but do appear as a common feature in computer models [29, 30] trying to describe the evolution of Universe.

Nearby dwarf spheriodal galaxies present an excellent target for DM searches. These clusters of stars, self gravitate and form coherent objects in orbit about the Milky Way. By measuring the motion of the stars within a dSph, astronomers can determine the total gravitating mass and this can be compared with the mass estimate derived by simply counting the stars. This is often expressed by the mass-to-luminosity ratio (M/L). Hence the DM within a dSph is "calibrated". In the most promising candidates this ratio exceeds 1000:1 albeit sometimes with large errors and many have a ratio exceeding 100:1 [31].

The current LAT search for a DM signal in dSphs uses a selection of 10 dSphs [32]. These dSphs are located within 150 kpc of the Sun and are $> 30°$ from the Galactic plane. These criteria are imposed to maximize any signal as well as reduce the foreground from the DGE.

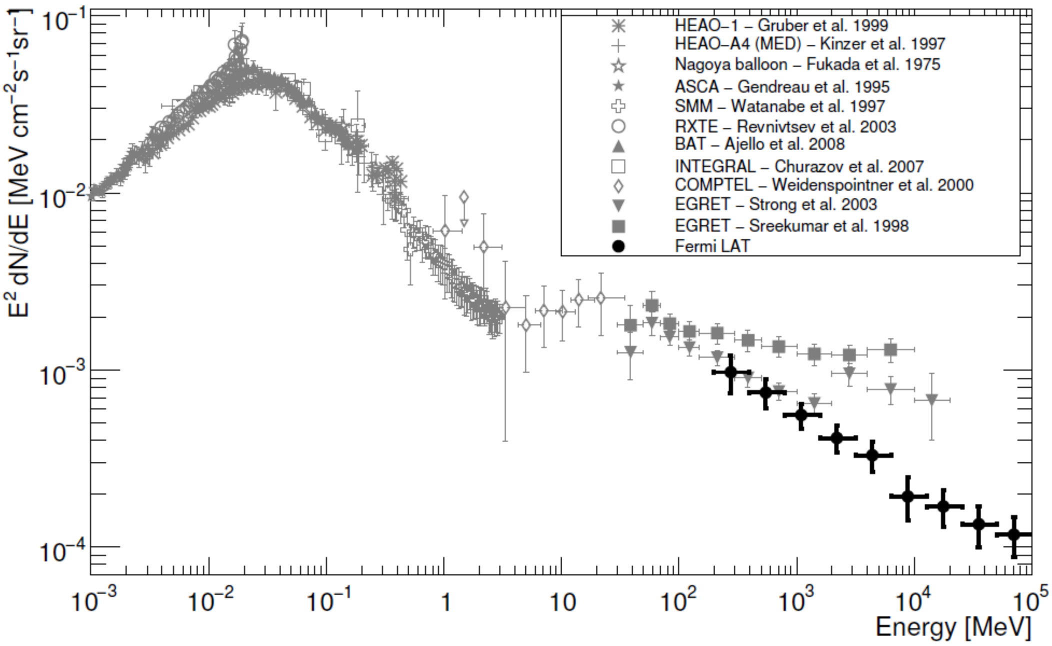


Figure 8: Spectral energy distribution of the extragalactic diffuse emission between 1 keV and 100 GeV measured by various instruments, including the *Fermi* LAT. Adapted from [24]. For full details of the LAT-derived spectrum see [25].

Using the first 9 months of data, no significant detection of these 10 objects is obtained, even before imposing a requirement that the spectra are DM-like. The 95% flux limits integrated above 100 MeV are at the $\sim 2-3\times10^{-9}$ ph cm$^{-2}$ s$^{-1}$ level and these will slowly improve over time.

Large $N$-body simulations predict that the distribution of DM will tend to clump as opposed to remain uniformly distributed within a galaxy. The simulations predict a distribution of masses for these clumps with the frequency of clumping increasing as the size of the clump becomes smaller. Overall, the predicted total rate for DM annihilations could be boosted by factors of a few, to more than an order of magnitude, over a uniform distribution. The rate at which these clumps might be found in $\gamma$-rays is very model dependent. Overall, 1-to-2 might be seen by the LAT with a one year exposure of the sky.

Such clumps would appear as unassociated $\gamma$-ray sources, with a spectrum characteristic of the annihilation process. If close by, they would also appear to be spatially extended. Currently, searches are under way with the LAT data for such occurances. The search criteria are 1) no counterpart observed close to the candidate location, 2) the emission is constant in time, 3) they be spatially extended ($\sim 1^\circ$), and 4) their spectrum is consistent with expectations for $\gamma$-rays from DM. After 10 months of data, the most promising of such unidentified sources has started to become resolved into two nearby sources. Hence, no claims for a significant detection for DM clumps is made by the LAT Collaboration. As more data is accumulated, the same criteria will be applied to subsequently detected unidentified sources.

*Galaxy Clusters:* Another “calibrated” DM source are galaxy clusters. Galaxy clusters are the most massive collapsed structures in the Universe where, from measurements of the relative motion of the galaxies about each other, the presence of large amounts of matter not traced by the individual galaxies is inferred. The LAT Collaboration has searched for a DM signal in the Coma and Fornax clusters, respectively [33]. However, as with the other promising targets, no signal in $\gamma$-rays has been observed.

## 4 Summary

The search for DM remains just that: a search. Exciting hints of signals have not stood up to closer examination with new, high precision experiments. Exhaustive searches in what should be the most promising channel, $\gamma$-rays, have so far turned up nothing that cannot be explained within “standard” astrophysics. However, it is also the case that when the $\gamma$-ray searches are turned into limits, the excluded parameter space does not place strong excludsions on models of DM based on extensions to the Standard Model. The limits will improve slowly over time, but likely will only be extended by a factor of a few.

The resolution to the real nature of the unobserved gravitating matter that so dominates our universe still awaits us. Perhaps with the extended high-energy reach afforded by the Large Hadron Collider (LHC) at CERN, some answers will be forth coming. Prior to the launch of *Fermi* many of us thought that the LHC would find candidate DM particles, providing details as to mass, cross sections, and inclusive branching fractions. Then armed with this knowledge *Fermi* LAT would map out the role the DM plays in the cosmos. It could very well play out this way, in spite of the delays in the commencement of data taking at the LHC. It could also turn out that the LHC finds no candidates and if this should be the case it is essential to recall that one of the most important experiments in Physics was a null experiment: the Michelson–Morley experiment preformed in 1887 [34]!

## 5 Acknowledgments

The author gratefully acknowledges the many contributions to this review and also the help in its preparation. In particular, to Simona Murigia for insights and critical comments and to Troy Porter for many useful discussions as well as help in the preparation of this manuscript.

The *Fermi* LAT Collaboration acknowledges generous ongoing support from a number of agencies and institutes that have supported both the development and the operation of the LAT as well as scientific data analysis. These include the National Aeronautics and Space Administration and the Department of Energy in the United States, the Commissariat à l’Energie Atomique and the Centre National de la Recherche Scientifique / Institut National de Physique Nucléaire et de Physique des Particules in France, the Agenzia Spaziale Italiana and the Istituto Nazionale di Fisica Nucleare in Italy, the Ministry of Education, Culture, Sports, Science and Technology (MEXT), High Energy Accelerator Research Organization (KEK) and Japan Aerospace Exploration Agency (JAXA) in Japan, and the K. A. Wallenberg Foundation, the Swedish Research Council and the Swedish National Space Board in Sweden.

Additional support for science analysis during the operations phase is gratefully acknowledged from the Istituto Nazionale di Astrofisica in Italy and the Centre National d’Études Spatiales in France.

# References


[1] V. C. Rubin *et al.*, ApJ **238**, 471 (1980).

[2] M. Markevitch *et al.*, ApJ **606**, 819 (2004).

[3] J. Chang *et al.*, Nature **456**, 362 (2008).

[4] O. Adriani *et al.*, Nature **458**, 607 (2009).

[5] W. B. Atwood *et al.*, ApJ **697**, 1071 (2009).

[6] A. A. Abdo *et al.*, PRL **102**, 181101 (2009).

[7] A. A. Abdo *et al.* PRL **103**, 251101 (2009).

[8] D. Grasso *et al.* APh **32**, 140 (2009).

[9] J. Nishimura *et al.*, ApJ **238**, 394 (1980).

[10] T. Kobayashi *et al.*, ApJ **601**, 340 (2004).

[11] F. A. Aharonian *et al.*, A&A **294**, L41 (1995).

[12] T. A. Porter & R. J. Protheroe, J.Phys.G **23**, 1765 (1997).

[13] M. K. Pohl & J. A. Esposito *et al.*, ApJ **507**, 327 (1998).

[14] F. A. Aharonian *et al.*, PRL **101**, 261104 (2008).

[15] F. A. Aharonian *et al.*, ApJL **696**, 150 (2009).

[16] C. S. Shen, ApJL **162**, 181 (1970).

[17] S. Profumo, arXiv:0812.4457 (2008).

[18] A. Arvanitaki *et al.*, PRD **80**, 055011 (2009).

[19] S. D. Hunter *et al.*, ApJ **481**, 205 (1997).

[20] W. de Boer, A&A **444**, 51 (2005).

[21] A. W. Strong, I. V. Moskalenko, & O. Reimer, ApJ **537**, 763 (2000).

[22] I. V. Moskalenko *et al.*, NuPhS **173**, 44 (2007).

[23] F. W. Stecker *et al.*, APh **29**, 25 (2008).

[24] M. Ackermann, on behalf of the Fermi-LAT collaboration. Talk at TeVPA 2009.

[25] A. A. Abdo *et al.*, PRL (accepted) (2010).

[26] P. Sreekumar P *et al*, ApJ **494**, 523 (1998).

[27] A. W. Strong, I. V. Moskalenko, & O. Reimer, ApJ **613**, 956 (2004).

[28] D. Elässer & K. Mannheim, PRL **94**, 171302 (2005).

[29] V. Springel *et al.*, Nature **435**, 629 (2005).

[30] J. Diemand *et al.*, Nature **454**, 735 (2008).

[31] M. L. Mateo, ARA&A **36**, 435 (1998).

[32] A. A. Abdo *et al.*, ApJ (accepted) (2010).

[33] A. A. Abdo *et al.*, in preparation (2010).

[34] A. Michelson & E. Morley, Am.J.Sci **34**, 333 (1887).

## Discussion

**Guido Altarelli (Roma3/CERN):** I heard that people were excited about the release of new results from FERMI in August 2009. Are those results included in your presentation?
**Answer:** The LAT worked immediately upon activation in orbit: when we turned it on - there was the gamma ray sky! Our ground simulations and analysis prior to launch were sufficient to begin science operations directly after the check out period. The easiest targets for early science are sources as they distinguish themselves by their location in the sky. There are now more then a dozen papers on sources. The fundamental science topics however, often involve pushing the instrument to its performance limit and understanding backgrounds, particularly when dealing with extended or diffuse signals. We are now just starting to produce results on these and this work is reflected in my presentation here. We expect however, that this is just the beginning.
**Roger Wolf (Univ. Hamburg):** Could you comment on the discrepancies between LAT and EGRET data?
**Answer:** The EGRET experiment was initially conceived in 1968 and used technologies contemporary with experimental techniques in particle physics of the 1960's, e.g. its trigger spark chamber. These made the on-orbit calibration difficult to monitor and track and lead to efficiency corrections which could vary by almost a factor of 3. In addition EGRET never had a complete monte-carlo simulation with which to study backgrounds and acceptance, and instead relied on extensive test beam data taken at SLAC and elsewhere. In short, there were systematic problems that limited the quantitative results. While acknowledging these short comings, we nevertheless emphasize that EGRET was the "path-finder" without which the enthusiasm and rapid development of the next generation gamma ray satellite would not have happened. Fermi-LAT on the other hand is representative of contemporary practice in high energy particle physics, from the choice of technologies to the extensive use of standard simulation packages (i.e. GEANT4). In addition the simulations were extensively cross-checked in beam tests at CERN and elsewhere.